

# A Study of SVC's Impact Simulation and Analysis for Distance Protection Relay on Transmission Lines

Ngo Minh Khoa\*<sup>1</sup>, Nguyen Huu Hieu<sup>2</sup>, and Dinh Thanh Viet<sup>3</sup>

<sup>1</sup>Quynhon University, Quynhon city, Vietnam

<sup>2,3</sup>The University of Danang - University of Science and Technology, Danang city, Vietnam

---

## Article Info

### Article history:

Received: Feb 15, 2017

Revised: May 24, 2017

Accepted: Jun 9, 2017

### Keyword:

Distance relay

Measured impedance

Matlab/Simulink

SVC

Power transmission line

---

## ABSTRACT

This paper focuses on analyzing and evaluating impact of a Static Var Compensator (SVC) on the measured impedance at distance protection relay location on power transmission lines. The measured impedance at the relay location when a fault occurs on the line is determined by using voltage and current signals from voltage and current transformers at the relay and the type of fault occurred on the line. The MHO characteristic is applied to analyze impact of SVC on the distance protection relay. Based on the theory, the authors in this paper develop a simulation program on Matlab/Simulink software to analyze impact of SVC on the distance protection relay. In the power system model, it is supposed that the SVC is located at mid-point of the transmission line to study impact of SVC on the distance relay. The simulation results show that SVC will impact on the measured impedance at the relay when the fault occurs after the location of the SVC on the power transmission line.

Copyright © 2017 Institute of Advanced Engineering and Science.

All rights reserved.

---

## Corresponding Author:

Ngo Minh Khoa

Faculty of Engineering and Technology, Quynhon University

170 An Duong Vuong street, Quynhon city, Vietnam

Phone: +84 988 371 737

Email: ngominhkhoa@qnu.edu.vn

---

## 1. INTRODUCTION

Nowadays, Flexible Alternating Current Transmission System (FACTS) devices are applied to power systems in order to improve the transmission capacity of the lines, enhance the power system stability and provide the optimum utilization of the system capability [1], [2]. The measured impedance at the relay location is the basis of the distance protection operation. There are several factors affecting the measured impedance at the relay location as presented in [1], [2]. Some of these factors are related to the power system parameters prior to the fault instance, which can be categorized into two groups [3]-[5]. The first group is structural conditions, represented by the short circuit levels at the transmission line ends, whereas the second group is the operational conditions, represented by the line load angle and the voltage magnitude ratio at the line ends. However, with the presence of FACTS devices such as SVC in particular, the conventional distance characteristics such as MHO and Quadrilateral are greatly subjected to mal-operation in the form of over-reaching or under-reaching the fault point [6]-[8].

Generally three installation positions are considered for the SVC; at the near end bus, at the mid-point of the line and at the remote end bus [9], [10]. In the case of ends buses, SVC is not present in the fault loop and therefore not affecting the distance relay operation. When SVC is installed at the mid-point, if the fault locates between the relaying point and the midpoint, the SVC is not present in the fault loop, otherwise SVC would be included in the fault loop. When SVC is not present in the fault loop for zero fault resistance, the measured impedance is equal to the actual impedance of the line section between the relay and fault locations. On the other hand, when SVC is within the fault loop, even in the case of zero fault resistance, the measured impedance would be deviated from its actual value. Therefore, the conventional distance relays are exposed to the mal-operation, in the form of over-reaching or underreaching. In this case, the effect of SVC on the protective zones should be considered accurately [9]-[11]. Thus, it is essential to study effects of FACTS devices on the protective systems,

especially the distance protection, which is the main protective device at Extra High Voltage (EHV) level.

This paper presents the SVC impact analysis on the performance of distance protection relay on the power transmission line using Matlab/Simulink software. At first a review of the effects of a SVC connected at the midpoint of a transmission line on the performance of distance protection relays is presented. Followed by a detailed simulation study for various types of faults applied on a transmission line protected by distance relay. The rest of the paper is organized as follows. The MHO characteristic and SVC operation principle are explained in Section 2. In Section 3, SVC impact analysis to the distance relay is presented in detail. The simulation results, analysis and evaluation are also showed in this section. Finally, the conclusion of this paper is included in Section 4.

## 2. MHO CHARACTERISTICS AND SVC

### 2.1. MHO characteristics

MHO distance protection is based on an electrical measure of distance along a transmission line to a fault. The distance along the transmission line is directly proportional to the series electrical impedance of the transmission line ( $Z_L$ ) between busbar A and B as shown in Figure 1. The distance protection measures distance to a fault by means of a measured voltage to measured current ratio computation [12]. The philosophy of setting relay at Sonelgaz Group [2] is three forward zones ( $Z_1$ ,  $Z_2$  and  $Z_3$ ) for protection the line HV between busbar A and B with total impedance  $Z_{AB}$ .

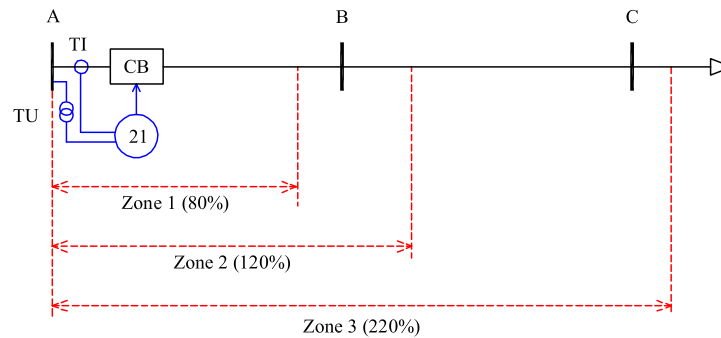


Figure 1. Setting zones of distance protection relay

The setting zones for protected transmission line without shunt FACTS devices are expressed by [11]-[15].

$$\begin{aligned} Z_1 &= 0.8Z_{AB} = 0.8(R_{AB} + jX_{AB}) \\ Z_2 &= R_{AB} + jX_{AB} + 0.2(R_{BC} + jX_{BC}) \\ Z_3 &= R_{AB} + jX_{AB} + 1.2(R_{BC} + jX_{BC}) \end{aligned} \quad (1)$$

where:

$Z_1$ ,  $Z_2$  and  $Z_3$ : The impedance of Zone 1, 2 and 3.

$R_{AB}$ ,  $X_{AB}$ : The resistance and reactance of the line AB.

$R_{BC}$ ,  $X_{BC}$ : The resistance and reactance of the line BC.

The total impedance ( $Z_{AB}$ ) of transmission line AB measured by the distance relay is given by:

$$Z_{meas} = K_Z Z_L = \left( \frac{K_{TU}}{K_{TI}} \right) Z_L \quad (2)$$

where:

$K_{TU}$ ,  $K_{TI}$  is the ratio of voltage and current transformers installed at the busbar A.

$Z_{meas}$  is the measured impedance from the relay to the fault location.

$Z_L$  is the actual impedance of line from the relay to the fault location.

### 2.2. The measured impedance at relay

This section considers the making of a distance relay by calculating the apparent impedance and comparing the result against some geometric shape. In this paper, we refer to this approach as the  $Z = V/I$  method. This

method is appealing in that it only requires one impedance calculation per fault loop. Multiple zones (or geometric shapes) only require more geometric tests of the result. These measured impedance equations are listed in Table 1.

Table 1. Apparent Impedance Equations [7]

| Fault type | $\dot{V}_R$                               | $\dot{I}_R$                               | $Z_{meas} = \dot{V}_R / \dot{I}_R$  |
|------------|---|---|---|
| AG         | $\dot{V}_a$                               | $\dot{I}_a + K\dot{I}_0$                  | $\dot{V}_a / (\dot{I}_a + K\dot{I}_0)$  |
| BG         | $\dot{V}_b$                               | $\dot{I}_b + K\dot{I}_0$                  | $\dot{V}_b / (\dot{I}_b + K\dot{I}_0)$  |
| CG         | $\dot{V}_c$                               | $\dot{I}_c + K\dot{I}_0$                  | $\dot{V}_c / (\dot{I}_c + K\dot{I}_0)$  |
| AB/ABG     | $\dot{V}_a - \dot{V}_b$                   | $\dot{I}_a - \dot{I}_b$                   | $(\dot{V}_a - \dot{V}_b) / (\dot{I}_a - \dot{I}_b)$   |
| AC/ACG     | $\dot{V}_a - \dot{V}_c$                   | $\dot{I}_a - \dot{I}_c$                   | $(\dot{V}_a - \dot{V}_c) / (\dot{I}_a - \dot{I}_c)$   |
| BC/BCG     | $\dot{V}_b - \dot{V}_c$                   | $\dot{I}_b - \dot{I}_c$                   | $(\dot{V}_b - \dot{V}_c) / (\dot{I}_b - \dot{I}_c)$   |
| ABC/ABCG   | $\dot{V}_a$ or $\dot{V}_b$ or $\dot{V}_c$ | $\dot{I}_a$ or $\dot{I}_b$ or $\dot{I}_c$ | $\frac{\dot{V}_a}{\dot{I}_a}$ or $\frac{\dot{V}_b}{\dot{I}_b}$ or $\frac{\dot{V}_c}{\dot{I}_c}$ |

where:

$\dot{I}_a, \dot{I}_b, \dot{I}_c$ : The current of phase A, B and C respectively.

$\dot{V}_a, \dot{V}_b, \dot{V}_c$ : The voltage of phase A, B and C respectively.

$\dot{I}_0 = (\dot{I}_a + \dot{I}_b + \dot{I}_c) / 3$ : The zero sequence current.

$K = (z_0 - z_1) / z_1$ .  $z_0, z_1$ : The zero-sequence and positive-sequence impedances of the line respectively.

### 2.3. Operation principle of SVC [6]

SVCs are devices that can quickly and reliably control line voltages. A SVC will typically regulate and control the voltage to the required set point under normal steady state and contingency conditions and thereby provide dynamic, fast response reactive power following system contingencies (e.g. network short circuits, line and generator disconnections). In addition, a SVC can also increase transfer capability, reduce losses, mitigate active power oscillations and prevent over-voltages at loss of load.

The SVC is customized to fit each customer with their specific needs. The SVC consists of a number of fixed or switched branches, of which at least one branch includes thyristors, and the combination of branches can be varied a lot depending on requirements. A SVC (Figure 2) typically includes a combination of at least two of the given items below (e.g. TCR/FC or TCR/TSC/FC): thyristor controlled reactor (TCR), thyristor switched capacitor (TSC), harmonic filter (FC) and Mechanically switched capacitor bank (MSC) or reactor bank (MSR) [6], [10].

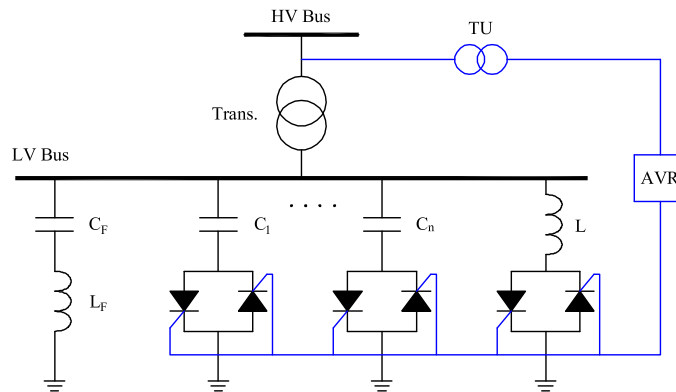


Figure 2. Simple control diagram of SVC [6]

## 2.4. Modeling of SVC

A typical terminal voltage versus output current of a static var compensator with a specific slope is shown in Figure 3. In most of applications, the static var compensator is not used as a perfect terminal voltage regulation, but rather the terminal voltage is allowed to vary in proportion with the compensating current. This regulation slope is defined as [6].

$$Slope = \frac{\Delta V_{C \max}}{I_{C \max}} = \frac{\Delta V_{L \max}}{I_{L \max}} \quad (3)$$

The regulation slope allows to extend the linear operating range of the compensator, to improve the stability of the voltage regulation loop and to enforce automatic load sharing between static var compensator as well as other voltage regulating devices.

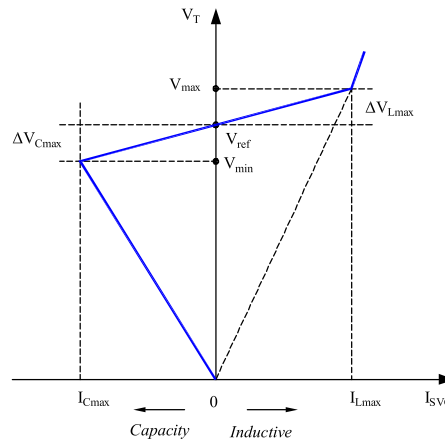


Figure 3. V-I characteristic of SVC

The voltage at which the static compensator neither absorbs nor generates reactive power is the reference voltage  $V_{ref}$  shown in Figure 3. In practice, this reference voltage can be adjusted within the typical range of 10%. The slope of the characteristic represents a change in voltage with compensator current and, therefore, can be considered as a slope reactance. The SVC response to the voltage variation is, then, determined from:

$$V_T = V_{ref} + X_{SL} I_{SVC} \quad (4)$$

Referring to Figure 3, the control range of a SVC is defined as follows [6]:

$$\begin{aligned} I_{\min} < I_{SVC} < I_{\max} \\ V_{\min} < V_{SVC} < V_{\max} \end{aligned} \quad (5)$$

In this range, the SVC is represented as a PV-node (generator node) at an auxiliary bus with  $P = 0$ ,  $V = V_{ref}$ . A reactance of ( $X_{SL}$ ) equivalent to the slope of the V-I characteristic is added between the auxiliary node and the node of coupling to the system. The node at the point of common coupling is a PQ-node with  $P = 0$ ,  $Q = 0$ , shown in Figure 4.

When SVC operates outside the control range, it is represented as a shunt element with the susceptance ( $jB$ ) on the operating point (see Figure 4.b),  $B$  is defined as:

$$\begin{aligned} \text{If } V < V_{\min} : \quad B &= \frac{1}{X_C} \\ \text{If } V > V_{\max} : \quad B &= -\frac{1}{X_L} \end{aligned} \quad (6)$$

where  $X_C$  and  $X_L$  are the reactances of the capacitor and reactor, respectively.

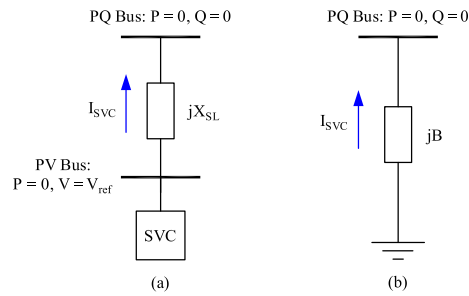


Figure 4. Equivalent model of SVC

### 3. SVC'S IMPACT ANALYSIS TO DISTANCE RELAY

#### 3.1. The studying power system model

Matlab is a high-performance language for technical computing. It integrates computation, visualization, and programming in an easy-to-use environment where problems and solutions are expressed in familiar mathematical notation. It is also applied in computing electrical engineering problems such as power quality analysis [16]-[18], modeling protection relays in power systems [19]-[20], etc. Therefore, to test and analyze the impact of SVC when a fault occurs on the power transmission line, the authors have developed a computer simulation program using Matlab GUI shown in Figure 5 to simulate the operation of distance protection relays in the power systems. In this model, the power system elements have the parameters as shown in Table 2.

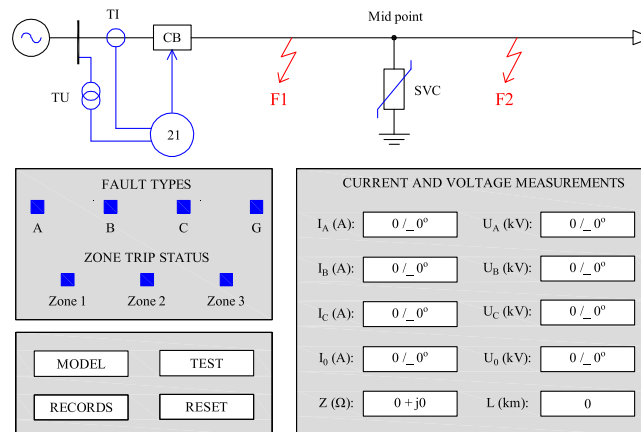


Figure 5. Distance relay simulation model with SVC in Matlab

The transmission line in the model is protected by the distance relays at the ends of the line and the SVC is located at the mid-point of the protected line. It is assumed that there are two fault locations which occur on the line including F1 (before SVC's location) and F2 (after SVC's location). Depending on the type of fault, the relay will determine the current and voltage signals from the current transformers and voltage transformers. Then, the measured currents at relay are compared to the current thresholds to identify the fault type and the measured impedance from the relay location to the fault location is also determined from the measured current and voltage. Finally, the relay will determine the fault which zone of MHO characteristic the fault belongs to. The main display functions on the graphical user interface are as follows:

- + **A, B, C** and **G**: The signals of fault type identification on the faulted phases A, B, C and G respectively.
- + **Zone 1, Zone 2** and **Zone 3**: The signals of Zone 1, Zone 2 and Zone 3 respectively.
- + **IA, IB, IC** and **I0**: The measured current on the phase A, B, C and zero-sequence at the relay location respectively.
- + **UA, UB, UC** and **U0**: The measured voltage on the phase A, B, C and zero-sequence at the relay location respectively.
- + **Z**: the measured impedance at the relay location.
- + **L**: The fault location on the transmission line.

Table 2. The Element Parameters

| Element           | Parameters                                       |
|-------------------|--|
| Source            | $f = 50$ (Hz); $V_{LL} = 220$ (kV)               |
|                   | $S_N = 9000$ (MVA); $X/R = 1$                    |
| Transmission line | $z_1 = 0.01273 + j0.2933$ ( $\Omega/\text{km}$ ) |
|                   | $z_0 = 0.3864 + j1.2963$ ( $\Omega/\text{km}$ )  |
|                   | $C_1 = 12.74 \cdot 10^{-9}$ (F/km)               |
|                   | $C_0 = 7.751 \cdot 10^{-9}$ (F/km)               |
|                   | $L = 200$ (km)                                   |
| SVC               | $V_{LL} = 220$ (kV)                              |
|                   | $Q_{SVC} = [-200 \div 200]$ (MVAR)               |

- + **MODEL**: The button to open the three-phase system.
- + **TEST**: The button to run the program.
- + **RECORDS**: The button to record the simulation results.
- + **RESET**: The button to reset the program to the initial values.

### 3.2. Response of SVC for faults

Assuming an one-phase to ground fault occurs on the line, the parameters of the SVC is shown in Figure 6. In normal operation mode before fault (0-5s), the voltage on the SVC is the rated voltage value (1.0 pu) shown in Figure 6(a). The value of the SVC substance is negative as shown in Figure 6(b), which shows the power system with capacitive properties. The SVC consumes a small amount of reactive power from the system  $Q_{SVC} > 0$  shown in Figure 6(c). When the fault occurs (at 5 seconds), the voltage of SVC rapidly decreases to zero shown in Figure 6(a). The value of SVC substance increases to 1 p.u shown in Figure 6(b). However, since the terminal voltage of SVC is decreased to zero, there is no reactive power of SVC generated or consumed shown in Figure 6(c).

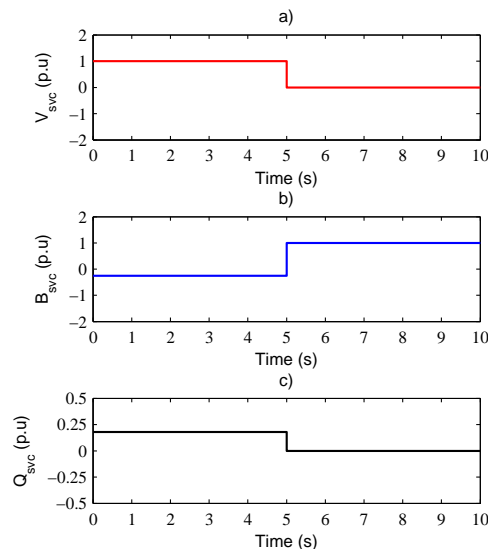


Figure 6. The SVC's parameters for one-phase to ground fault at location 100 km on the transmission line

### 3.3. Measured impedance at relay with/without SVC

It is assumed that the fault types occurring at different locations on the transmission line are in turn separated by a distance of 20 km from the relay location. Table 3 shows the simulation results of measured impedance

at the relay location with and without SVC which is connected at mid-point of the line.

Table 3. Measured Impedance for Fault Types

| Fault location (km) | Actual Impedance $Z_{act}$ ( $\Omega$ ) | Measured impedance $Z_{meas}$ ( $\Omega$ ) |        |        |        |          |        |        |        |
|---------------------|---|--|--------|--------|--------|----------|--------|--------|--------|
|                     |   | Without SVC                                |        |        |        | With SVC |        |        |        |
|                     |   | LLLG                                       | LL     | LLG    | LG     | LLLG     | LL     | LLG    | LG     |
| 20                  | 5.872                                   | 5.873                                      | 5.878  | 5.878  | 5.872  | 5.874    | 5.873  | 5.873  | 5.869  |
| 40                  | 11.744                                  | 11.745                                     | 11.752 | 11.887 | 11.743 | 11.75    | 11.752 | 11.752 | 11.733 |
| 60                  | 17.616                                  | 17.611                                     | 17.599 | 17.685 | 17.615 | 17.641   | 17.641 | 17.641 | 17.597 |
| 80                  | 23.489                                  | 23.483                                     | 23.393 | 23.404 | 23.49  | 23.546   | 23.548 | 23.548 | 23.456 |
| 100                 | 29.361                                  | 29.359                                     | 29.334 | 29.251 | 29.364 | 29.477   | 29.476 | 29.476 | 29.321 |
| 120                 | 35.233                                  | 35.233                                     | 35.256 | 35.169 | 35.225 | 35.578   | 35.581 | 35.581 | 36.083 |
| 140                 | 41.105                                  | 41.104                                     | 41.219 | 41.119 | 41.108 | 42.036   | 42.035 | 42.035 | 43.179 |
| 160                 | 46.977                                  | 46.958                                     | 47.112 | 47.058 | 46.987 | 48.874   | 48.876 | 48.876 | 50.614 |
| 180                 | 52.849                                  | 52.844                                     | 52.835 | 52.95  | 52.768 | 56.145   | 56.147 | 56.147 | 58.369 |
| 200                 | 58.721                                  | 57.706                                     | 58.806 | 58.773 | 58.829 | 63.896   | 63.896 | 63.896 | 66.346 |

The results in Table 3 show that when a fault occurs at the particular location on the line with any types of fault, the relay also determines the same measured impedance. Therefore, the fault location will be determined as the same result. However, if a SVC is connected to mid-point of the line, the measured impedance at the relay will have different results comparing to the without SVC case. This simulation result is shown in Figure 7. In Figure 7, the trajectory of measured impedance at the relay when a one-phase to ground fault occurs at the location 120 km on the line calculated from the relay location. The results show that if there is no SVC, the measured impedance point will belong to Zone 2 of MHO characteristic, but if the SVC is connected to the mid-point of line, the measured impedance at the relay location will belong to Zone 3.

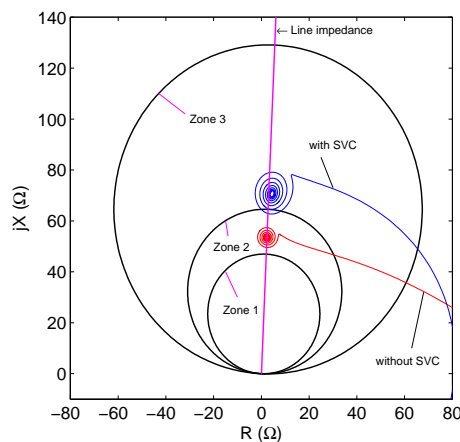


Figure 7. Apparent impedance with SVC at mid-point of the line

In order to evaluate the error between the measured impedance at the relay location and the actual impedance of the line calculated from the relay location to the fault location, this paper proposes an error which is given as follows:

$$Error\% = \frac{Z_{meas} - Z_{act}}{Z_{act}} 100 \quad (7)$$

The percentage error result of the measured impedance for all fault types which occur at the different locations on the line in two cases including with and without SVC is shown in Figure 8. For all fault types, if the location is before SVC location, the SVC will not affect the measured impedance at the relay. So the measured impedance in both cases (without SVC and with SVC) is almost equal as shown in Figure 8 (from 0-100 km). If a fault occurs after the SVC location, the measured impedance at the relay in both two cases is different. Specifically, the measured impedance with SVC will be much larger than the measured impedance without SVC in the same location as shown in Figure 8 (from 100 to 200 km). So when there is a fault occurring in the location before it has errors SVC impedance measuring nearly 0 even when there is a fault occurring and farther behind SVC placement, the level of total return measured error will be greater.

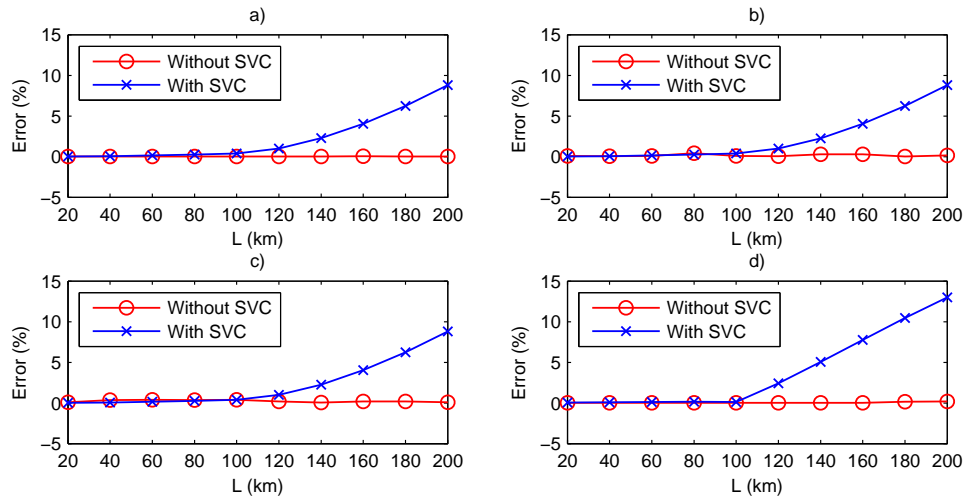


Figure 8. Error of measured impedance at relay for fault types at different locations. a) Three-phase to ground fault, b) Phase to phase fault, c) Two-phase to ground fault, d) Phase to ground fault

Fault resistances affect the measured impedance at the relay because they can make the voltage and current at the relay different with the direct fault without resistance. So this paper also studied the impact of the fault resistance on the distance relay as shown in Figure 9. Figure 9(a) shows the error of the measured impedance at the relay when direct faults occur at different locations on the line. It clearly shows that the error depends on the fault resistance and location. When SVC is connected to mid-point of the line, the error increases significantly for faults occurring after the SVC location as shown in Figure 9(b).

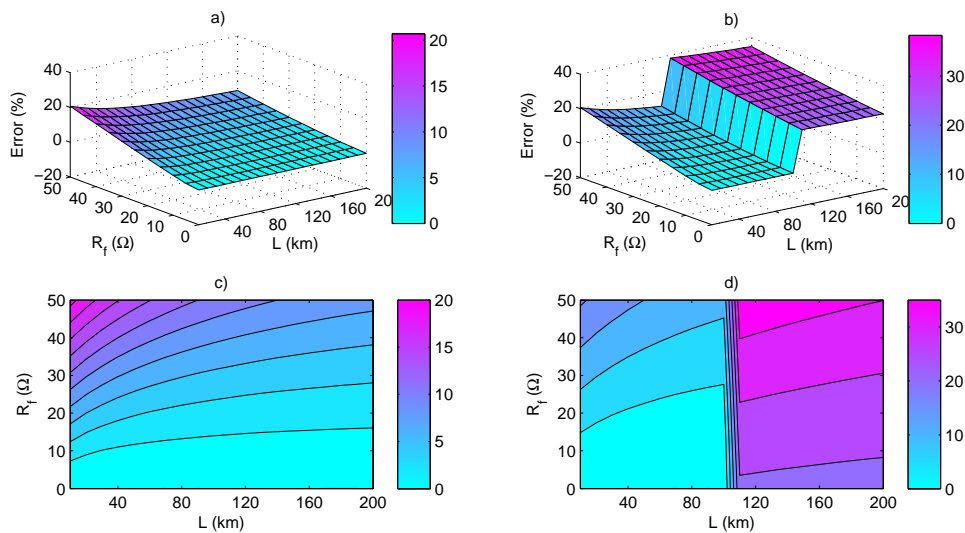


Figure 9. Error of measured impedance at relay according to the fault resistances and locations. a-b) The 3D plots of the error without and with SVC, c-d) The contour plots of the error without and with SVC

**4. CONCLUSION**

This paper studies the influence analysis of SVC to the measurement impedance determination of the distance protection relay in the power system. The voltage and current measured at the relay location depend on the faults' location and type which occur on the transmission line. Then the measured impedance is determined from these signals. MHO characteristic is used to determine the fault zone.

SVC is located at the mid-point of the power transmission line to analyze and evaluate in this paper. From the simulation model built on Matlab/Simulink software, this paper has analysed and showed that the SVC will

affect the measured impedance at distance protection relay if the fault occurs after SVC's location. SVC can make the position of the fault fall in the different zones other than the case of without SVC. This can make the trip signal incorrectly and not guarantee the selective feature of the relay.

## REFERENCES

- [1] A. Kazemi, S. Jamali and H. Shateri, "Measured Impedance by Distance Relay in Presence of SVC on Transmission Line," *International Review of Electrical Engineering*, 2006; 5: 2214-2219, 2006.
- [2] Mohamed Zelligui and Abdelaiz Chaghi, "Impact of SVC Devices on Distance Protection Settings Zones in 400kV Transmission Line," *UPB Scientific Bulletin, Series C: Electrical Engineering*, Vol. 75, Iss. 2, pp. 249-262, 2013.
- [3] Azriyenni Azriyenni, Mohd Wazir Mustafa, "Application of ANFIS for Distance Relay Protection in Transmission Line," *International Journal of Electrical and Computer Engineering*, Vol. 5, No. 6, pp. 1311-1318, 2015.
- [4] A N Sarwade, P K Katti, J G Ghodekar, "Reach and Operating Time Correction of Digital Distance Relay," *International Journal of Electrical and Computer Engineering*, Vol. 7, No. 1, pp. 58-67, 2017.
- [5] Aejaaz Ahmed K R, Mohd. Z. A. Ansari, Mohamed Jalaluddin, "Simulation Analysis of a Power System Protection using Artificial Neural Network," *International Journal of Electrical and Computer Engineering*, Vol. 3, No. 1, pp. 78-82, 2013.
- [6] M. Noroozian, *Modelling of SVC in Power System Studies*, ABB Power Systems, 1996.
- [7] Ahmed Kareem Lafta Al-Behadili, *Performance Analysis of Distance Relay on Shunt/Series Facts-Compensated Transmission Line*, Master's Theses, Western Michigan University, 2015.
- [8] Carson W. Taylor, "Static Var Compensator Models for Power Flow and Dynamic Performance Simulation," *IEEE Trans. on Power Systems*, Vol. 9, No. 1, pp. 229-240, 1994.
- [9] F.A. Albasri; T.S. Sidhu; R.K. Varma, "Impact of Shunt-FACTS on Distance Protection of Transmission Lines," *Power Systems Conf.: Adv. Metering, Protection, Control, Communication, and Distributed Resources*, pp. 249-256, 2006.
- [10] F.A. Albasri, T.S. Sidhu, R.K. Varma, "Mitigation of Adverse Effects of Midpoint Shunt-FACTS Compensated Transmission Lines on Distance Protection Schemes," *Power Engineering Society General Meeting*, pp 1-8, 2007.
- [11] Sabyasachi Behera; P. Raja; S. Moorthi, "Modelling and simulation of the impact of SVC on existing distance relay for transmission line protection," *2015 International Conference on Condition Assessment Techniques in Electrical Systems (CATCON)*, pp. 151-156, 2015.
- [12] Xiao-Ping Zhang, Christian Rehtanz, Bikash Pal, *Flexible AC Transmission Systems: Modelling and Control (Power Systems)*, 2nd ed. 2012 Edition, Springer, 2012.
- [13] Amir Ghorbania, Mojtaba Khederzadehb, Babak Mozafaria, "Impact of SVC on the protection of transmission lines," *International Journal of Electrical Power and Energy Systems*, Vol. 42, Iss. 1, pp. 702-709, 2012.
- [14] David G Philip; Arun Rajendran, "Numerical conic distance relay," *2015 International Conference on Innovations in Information, Embedded and Communication Systems (ICIIECS)*, pp. 15, 2015
- [15] David G Philip; Arun Rajendran, "Development of a Multi-characteristic Distance Relay," *2015 International Conference on Technological Advancements in Power and Energy (TAP Energy)*, pp. 176-181, 2015.
- [16] Dinh Thanh Viet, Nguyen Huu Hieu, Ngo Minh Khoa, "A Method for Monitoring Voltage Disturbances Based on Discrete Wavelet Transform and Adaptive Linear Neural Network," *International Review of Electrical Engineering*, Vol. 11, No. 3, pp. 314-322, 2016
- [17] Dinh Thanh Viet, Nguyen Huu Hieu, Nguyen Le Hoa, Ngo Minh Khoa, "A Control Strategy for Dynamic Voltage Restorer," *Proceedings of The 11th IEEE International Conference on Power Electronics and Drive Systems (PEDS 2015)*, 9 - 12, Sydney, Australia, June 2015.
- [18] Ngo Minh Khoa, Dinh Thanh Viet, Nguyen Huu Hieu, "Classification of Power Quality Disturbances Using Wavelet Transform and K-Nearest Neighbor Classifier," *Proceedings of The 22nd IEEE International Symposium on Industrial Electronics (ISIE 2013)*, Taipei, Taiwan, May 2013.
- [19] Li-Cheng Wu; Chih-Wen Liu; Ching-Shan Chen, "Modeling and testing of a digital distance relay MATLAB/SIMULINK," *Proceedings of The 37th Annual North American Power Symposium*, pp. 253-259, 2005.
- [20] Nur Hazwani Hussin; Muhd Hafizi Idris; Melaty Amirruddin; Mohd Saufi Ahmad; Mohd Alif Ismail; Farrah Salwani Abdullah; Nurhakimah Mohd Mukhta, "Modeling and simulation of inverse time overcurrent relay using Matlab/Simulink," *Proceedings of 2016 IEEE International Conference on Automatic Control and Intelligent Systems (I2CACIS)*, pp. 40-44, 2016.

**BIOGRAPHIES OF AUTHORS**

**Ngo Minh Khoa** received the MS and PhD degrees in Electrical Engineering from The University of Danang - University of Science and Technology, Danang City, Vietnam, in 2010 and 2017, respectively. He is currently teaching at Quynhon University, Quynhon city, Vietnam. His research interests include protection relay, power quality, and smart grid.



**Nguyen Huu Hieu** received PhD degree in Electrical Engineering from Joseph Fourier, Grenoble, France in 2008. He is currently Dean of Electrical Engineering Department, The University of Danang - University of Science and Technology, Danang city, Vietnam. His research interests include power quality, optimization method, and power system design.



**Dinh Thanh Viet** received PhD degree in Electrical Engineering from Vinnitsya Technical State University, Ukraine in 1997. Currently he is Associate Professor at Department of Electrical Engineering, The University of Danang - University of Science and Technology, Danang city, Vietnam. His research interests include power system analysis and control, power quality, transformer diagnosis, and deregulated market.